BSPE 00572-896-7

한국 심해연구지역 주상 퇴적물중 희토류 원소 함량 특성

Geochemistry of rare earth elements in two-colored core sediments from the Korea Deep Ocean Study (KODOS)-90 area, western part of Clarion-Clipperton fracture zone, northeast equatorial Pacific

1996. 3

한 국 해 양 연 구 소

제출문

한국해양연구소장 귀하

본 보고서를 "한국 심해연구지역 주상 퇴적물중 희토류 원소 함량 특성" 연구사업의 최종보고서로 제출합니다.

1996년 3월

한 국 해 양 연 구 소

연구책임자 : 정회수
이경용
연구원 : 김채수

요 약 문

I. 제 목

한국 심해연구지역 주상 퇴적물중 희토류 원소 함량 특성

II. 연구개발의 내용 및 결과

본 연구는 북동 태평양 클라리온-클리퍼톤 균열대지역 (Clarion-Clipperton fracture zone, C-C zone) 사이에 위치한 한국심해연구 (Korea Deep Ocean Study Area, KODOS) 지역에서 1990년 10 개 정점에서 채취된 주상 퇴적물중 희토류 원소 (Rare Earth Elements, REE)의 수직분포 특성에 관한 것이다. 연구 목적은 연구지역에서 나타나는 퇴적물 색상 경계면을 중심으로 희토류원소의 함량이 크게 다른 원인을 구명코자 함이다. 이를 위해 두가지 색상 퇴적물중 금속 및 방사능 원소 함량, 미세망간단괴 (micronodule)등을 포함한 각종 조립 입자의 조성 분석, 점토광물 조성 및 함량 분석 등을 실시하였다.

연구지역 퇴적물에 나타나는 희토류 원소의 함량 특성은 주로 퇴적물에 포함된 Ca-P화합물에 의해 조절됨을 알 수 있었다. Ca-P

화합물의 높은 함량은 퇴적 당시의 고해양환경 (paleoceanography) 변화 즉 마이오세 말기 퇴적결층인 색상 경계면을 형성할 당시 강한 저층류 흐름을 가능케 한 지구 표면의 큰 온도 구배와 이에 따른 해양계의 증가된 생산력 (productivity)에 기인하였다.

SUMMARY

I. Title of the study

Geochemistry of rare earth elements in two-colored core sediments from the Korea Deep Ocean Study (KODOS) -90 area, western part of Clarion-Clipperton fracture zone, northeast equatorial Pacific

II. Abstract

To study the geochemistry of rare earth elements (REEs) in two-colored core sediments, ten box-core samples were sampled from the Korea Deep Ocean Study (KODOS) -90 site located at the western part of Clarion-Clipperton fracture zone, northeast equatorial Pacific. Topmost sediment column is divided into two layers by a sharp color boundary; an upper pale brown layer (unit A) and a lower dark brown layer (unit B). The color boundary is interpreted to be a hiatus formed by intensified paleo- bottom currents based on the excess activities of ^{230}Th and the assemblage

of Quaternary and Tertiary radiolarians. Contents of REEs as well as fish remains, smectite aggregates, micronodules, heavy metals (Mn, Cu, Ni), smectite, and severely deteriorated fossils (spicules and spines) are high just below the hiatus.

REEs are not concentrated in the particles such as micronodules, smectite aggregates, and smectite, etc.. On the other hand, they are highly concentrated in the fish remains that was identified to be Ca-P composites. A large amount of fish remains was expected to be supplied to the sea bottom when the productivity in water column was high. Productivity during the period of the hiatus was probably high for the glaciation of the Antarctic region and steep temperature gradient on earth surface. Moreover, the intensified bottom currents could promote the reworking and winnowing processes, and concentrate the coarse grains such as fish remains, micronodules, and smectite aggregates just below the hiatus. It is suggested that the enrichment of REEs in the upper part of unit B was due to the fish remains abundant just below the color boundary. In addition, abundant supply of the remains was probably responsible for the great changes in paleoceanography (i.e., paleo- climatology) during the formation of the hiatus.

Contents

List of Tables

List of Figures

Fig. 9 Contents of smectite in fine fraction (>2 μm) of unit A (filled circle) and unit B (open triangle) sediments in KODOS-90 site

Fig. 10 Depth profiles of Ce anomalies (Ce/Ce*) in box core sediments from KODOS-90 site. Ce/Ce* values decrease abruptly across the color boundary in st.14, st.34, st.36, and st.37

Fig. 11 REE contents in unit A, unit B, smectite, micronodules, smectite aggregates, and fish remains in box core sediments from KODOS-90 site. Note the enriched REEs in fish remains.

I. Introduction

Rare earth elements (REEs) have been used as an useful tool for the understanding of geochemical processes because of their similar chemical properties and the low solubilities (Piper, 1974; Toyoda et al., 1990). Diagenetic remobilization of REEs in marine anoxic sediments is another important process discussed severely in recent (Elderfield et al., 1981b; Elderfield and Sholkovitz, 1987; Murray et al., 1991).

One of the hot issues on REE geochemistry is the assessing and ranking the controlling parameters of REE contents in marine sediments (Murray et al., 1991). Hydrothermal input, diagenetic process, and the input of biogenic particles control the REE composition of deep sea sediments (Piper et al., 1974; Elderfield et al., 1981a; Toyoda et al., 1990). It is well known that REEs are highly concentrated in manganese nodules with positive Ce anomaly and in philipsite with strong negative Ce anomaly, while they are depleted in foraminifera and calcite (Piper, 1974; Elderfield et al., 1981). Toyoda et al. (1990) reported that fish bone debris readily accumulates REE with a large negative Ce anomaly in the central equatorial Pacific.

The Korea Deep Ocean Study (KODOS) programme has been carried out since 1989 by the Korea Ocean Research and Development Institute (KORDI) for the environmental research and manganese nodule exploration in KODOS area, western part of Clarion-Clipperton fracture zone (C-C zone) in the northeast equatorial Pacific. Based on the detailed analysis on core sediments at the KODOS-89 and -90 sites, it was found that REE contents as well as other geochemical and mineralogical properties in two-colored core sediments are clearly different across a color boundary between the upper light brown and the lower dark brown layers

(KORDI, 1991; Jung, 1994).

In this report, a primary controlling parameter for the vertical variation of REEs across the boundary is discussed from the chemistry of bulk sediments and their components.

II. Regional setting

KODOS-90 site is located between 146~153 °W and 7~12 °N in the western margin of the C-C zone (Fig. 1). Abyssal plain with 5,100~5,300 m in water depth is widely spread over the study area with several seamounts on the plain. Radiolaria-bearing siliceous sediments are distributed dominantly in the study area despite of occasional occurrence of calcareous ooze on seamounts (Jung et al., 1991; KORDI, 1991).

In the C-C zone, sedimentation rates are variable from less than 0.5 mm/10^3 yr to several mm/10^3 yr (Piper, 1977; Muller and Mangini, 1980; Halbach et al., 1988; KORDI, 1991). Local redistribution of sediments by bottom currents is an important factor for the large variation of the sedimentation rates (Piper and Blueford, 1982; Skornyakova and Murdmaa, 1992). Antarctic bottom water (AABW) characterized by high oxygen contents and low temperature passes northeastwards through the Line Island chain and then spreads over the nodule belt of C-C zone (Johnson, 1972; Halbach et al., 1988; Gordon and Gerard, 1970). Invasion of the intensified AABW flow in the northeast Pacific is indicated by the hiatus of the late Tertiary (Halbach et al., 1988).

A hiatus between the Quaternary and the Tertiary occurring

frequently in the north Pacific was created by the intensified AABW flow during the middle Miocene to the early Pliocene (Halbach et al., 1988; Jeong et al., 1994). The AABW flow, which was stronger than the present AABW flow, was formed due to the onset of major glaciation of Antarctica during the late Miocene (Johnson, 1972; Savin et al., 1975; van Andel et al., 1975; Halbach et al., 1988). Meanwhile, sedimentation in the equatorial Pacific during the Quaternary and the Tertiary was affected nearly continuously by two processes of reworking of older sediments and resedimentation (Halbach et al., 1988).

Most of the nodules occurring in the study area are 2~4 cm in diameter, ellipsoidal to discoidal in shape, and rough in surface texture (Jeong et al., 1994). The nodules are abundant (> 10 /m^2) on the seamount belt of 10 $^{\circ}$N region (Jung et al., 1990; Lee et al., 1992) due to the seeding effect of hydrogenetic nodule fragments created by the strong bottom currents (Jung et al., 1990; Lee et al., 1992). Meanwhile, it was suggested that redistributional processes of bottom currents seems to be most responsible for the regeneration and concentration of nodules in the KODOS -89 and -90 sites (Jeong et al., 1994).

III. Sampling and analytical methods

KODOS-90 site was surveyed during the corporation between KORDI and U.S. Geological Survey (USGS) using R/V Farnella in 1990 (Fig. 1). Ten box cores were collected using box corer, and subsamples were taken into polyprophylene bottles at predesigned depth intervals. Subsamples were stored in a refrigerator for the

additional analysis after sealing the bottles tightly with parafilm. Sediment slabs were obtained from the box core sediments using a transparent acrylic box with size of 20x35x2 cm, and was described after taking photograph of the slab.

Sediment subsamples were ground to pass 200 mesh nylon sieve after drying them in a oven under 80 ^{o}C for 24 hours. These sediment samples were digested with 4 ml, 3 ml, and 6 ml of concentrated HF, $HClO_4$, HNO_3, respectively, in a tightly-closed teflon vessel on a hot plate with temperature less than 150 ^{o}C for 24 hours (Kitano and Fujiyoshi, 1980). After eluting the white cake of digested sediments using 1 N HNO_3 solution, concentrations of Mn, Fe, Cu, Ni, and Co were measured with a flame atomic absorption spectrophotometer (AAS, Varian SPECTRAA-10). Concentration of REEs in the eluted solution was analyzed using inductively coupled plasma mass spectrometer (ICP-MS, VG element PQ-II). Meanwhile, BCSS-1 and MAG-1 standard reference sediments were analyzed simultaneously with KODOS sediments for the checking of data quality.

For the analysis of excess ^{230}Th activities (^{230}Th = ^{230}Th – ^{234}U), dried sediments (0.5 ~ 1.00 g) were digested with mixed solution of concentrated HCl, $HClO_4$, and HNO_3. After passing the digested solution through ion exchange column (Dowex AGI-X8, 100-200 mesh, chloride form), Th and U were electroplated for 60 ~ 90 minutes at 4 or 9 volts. Counting of uranium and thorium isotopes was done by alpha spectrometers with silicon surface-barrier detectors (Canberra, Oxford) mounted inside vacuum counting chamber.

For the grain size analysis, wet sediments were dispersed in 0.1 % $(Na_3PO_4)_6$ solution using an ultra sonic bath (50 W, 27 kHz) for 15 minutes after pretreating the sediments with concentrated

H_2O_2. Analysis was done using standard sieves (62 μm, 45 μm, 25 μm) and a laser-scattering particle size analyzer (MALVERN MasterSizer). Standard zircon grains (2 μm, 5 μm, 16 μm, MICROMERITICS) were used for the calibration of the grain size analysis (Jung et al., 1993).

Clay mineralogy was analyzed with X-ray diffractometer (XRD, Philips PW1710), after separating the clay grains (<2 μm) from bulk sediments using pipetting method (Brunton, 1955; Biscaye, 1965). Clay sediments (<2 μm) separated from bulk sediments were dried, weighed, and digested according to the above scheme for the analysis of REEs. REE contents in the clay samples were analyzed with a high resolution ICP-MS (VG element PLASMA TRACE).

Several hundreds of radiolaria, micronodules, and brown particles were separated from coarse fraction (> 25 μm) by hand using a plastic needle under a microscope equipped with a camera (Leitz Vario-Orthomat model). After collecting micronodules and brown particles to several milligrams, they were dried, weighed, and digested according to the analytical method of REEs. REE concentration was measured by high resolution ICP-MS. In addition, compositions of micronodules and brown particles were analyzed qualitatively by the energy dispersive spectrometry (EDS) method using a scanning electron microscope (SEM, Hitachi X-650) equipped with EDS system (KEVEX 7000). Meanwhile, radiolarian assemblages were identified after mounting coarse grains (> 62 μm) on a slide glass using the microscope.

IV. Results and Discussion

1. Geochronological and compositional characters in two-colored core sediments

All the core samples in the study area are composed mostly of siliceous clay with pale or dark brown color. A lot of bioturbation traces can be observed in the massive sedimentary column without sedimentary structure or laminae. The traces are different in color from surrounding matrices; that is, light yellow traces are embedded in the upper pale brown layer and pale brown traces are in the lower dark brown layer (Fig. 2). We can not find any systematic trend in the occurrence frequency of the traces with core depth.

Based on the variation of sediment color, core samples can be divided into two layers; an upper pale brown layer (unit A; 10YR 6/4~6/6; Munsell, 1988) and a lower dark brown layer (unit B; 10YR 4/3~3/3). Among ten cores, four cores (st. 14, 34, 36, 37) have a color boundary between unit A and B while the other cores are composed only of unit A (Table 1). These color boundaries were reported in the core sediments from the north Pacific (Piper and Blueford, 1982; von Stackelberg, 1982; Kadkho, 1985; Piper et al., 1987).

Excess ^{230}Th activities in unit A are evidently higher (about 100 dpm/g) than those in unit B (about 1 dpm/g) (Fig. 3). The abrupt decrease of ^{230}Th activity across the color boundary indicates that the boundary is a hiatus with an age difference of at least 0.5 Ma. The age difference between unit A and B can also be referred from radiolarian assemblages. Radiolaria is the most abundant and well-preserved microfossil in the study area compared to others such as silicoflagellate, coccolith, etc.. Quaternary radiolarians such as *Polysolenia spp., Anthocyrtidium spp., Spongaster t. dianae,* and

Artostrobium miralestense are ubiquitous in unit A while Tertiary or Quaternary~Tertiary groups (*Euchitonia sp., Spirocyrtis scalaria,* and *Theocampe mongolfieri*) occur scarcely. In unit B, however, Tertiary radiolarians such as *Theocampe mongolfieri, Thyrsocyrtis triacantha, Lithocyclia ocellus* and *Podocyrtis geotheana* occur frequently while Quaternary radiolarians are few. Occasional occurrence of Quaternary radiolarians in unit B is due to the pale brown burrow traces embedded in unit B. In DOMES site A lying near the study area (Fig. 1), the boundary was assigned to be a hiatus between the Quaternary and the Tertiary based on radiolarian assemblages (Piper and Blueford, 1982; Piper et al., 1987). In the central north Pacific, the boundary was reported to be a hiatus between the late Miocene to the Pliocene based on ^{10}Be activities of piston core sediments (Kadkho, 1985).

Grain size distribution of bulk sediments in the core top generally shows a bimodal pattern with a fine mode (60~70 ㎛) and a coarse mode (2~8 ㎛) (Fig. 4). The coarse mode disappears gradually with depth in unit A, and fine mode occurs solely in unit B. Although coarse grains (> 25 ㎛) are mostly composed of siliceous radiolarian tests and fragments in unit A sediments, coarse grained black micronodules, reddish yellow smectite aggregates, and water-white fish remains are also abundant in the upper part of unit B (Fig. 5, 6). Radiolarian tests in unit A are preserved well while severely deteriorated fossil fragments and spicules/spines are abundant in the upper part of unit B (Fig. 5, 6). The preservation state of the radiolarians in the lower part of unit B is better than that in the upper part of unit B (Fig. 5). EDS spectrum shows that the micronodule consists mostly of Mn with subordinate amount of Fe (Fig. 7). The brown (pale yellow brown or reddish yellow brown) particle shows an EDS spectrum with high peaks of Si, Fe and small peaks of Al, K, Ca (Fig. 7). The brown particle is regarded to

be Fe-rich smectite (or nontronite) aggregate because of its similar EDS spectrum to that of smectite (Fig. 7, 8; Welton, 1984). The aggregates were also found in the bottom sediments of the northwestern Pacific, and assigned to be smectite aggregates (Hein et al., 1979).

Clay minerals (<2 ㎛) are mostly composed of smectite and illite, and kaolinite+chlorite contents are negligible. Hence, depth profiles of illite shows a mirror image with those of smectite (Fig. 2). Smectite contents increase abruptly across the color boundary from approximately 45% in unit A to 80% in unit B (Fig. 9). Although we can not do a quantitative analysis on the composition of clay minerals, it seems that clay minerals are composed mostly of smectite in the upper part of unit B because smectite peak is nearly unique on the diffractogram while other peaks are negligible (Fig. 8).

All the sediment characters in unit A and B are summarized in Table 2 and Fig. 2.

2. Factors controlling the REE contents in unit A and B sediments

REE contents in KODOS sediments vary greatly with sampling location as well as with core depth (Table 3). Maximum values of REEs in the study site are 5 (Ce) to 26 times (La) greater than the minimum values (Table 4). Despite of the great difference, averaged REE contents are comparable in a order of magnitude to those in North American Shale Composites (NASC) (Table 4). All of the REEs except Ce are enriched in KODOS sediments (Table 4). Especially, heavy REEs are more enriched than light REEs (Table 4). Enrichment of the heavy REEs might be due to a lot of siliceous fossil tests in KODOS sediments. Siliceous organisms can uptake more amount of heavy REEs concentrated in sea water compared to light REEs that have shorter residence time than heavy REEs

(Henderson, 1984). Meanwhile, averaged Ce contents in KODOS sediments are lower than those in NASC (Table 4).

Although REE contents are nearly uniform with core depth in unit A, the contents (except Ce) increase abruptly across the color boundary (Table 2, 3; Fig. 2). All REE contents (except Ce) in unit B of st.14, st.34, st.36, st.37 are three or four times higher than those in unit A (Table 3). On the other hand, Ce contents in unit B are similar to those in unit A. Hence, Ce anomalies (Ce/Ce*) in unit A and B are clearly different, and decrease abruptly across the color boundary between unit A and B (Fig. 10).

Compositions of unit A and B sediments are different in many aspects. Micronodules are abundant and heavy metals (Mn, Cu, Ni) are enriched in unit B (Table 2, Fig. 2). Enrichment of heavy metals in unit B is due to the abundant micronodules (Jung et al., 1991). Compositions of micronodules are generally similar to those of manganese nodules which have high concentrations of Mn, Cu, Ni, etc.. (Jung, 1994; Addy, 1978). Meanwhile, it is well known that REE contents in manganese nodules are generally higher than those in deep sea sediments (Henderson, 1984). If REE contents in micronodules are also higher than those in deep sea sediments, enriched REEs in unit B might be due to the abundant micronodules in unit B. To check this probability, REE contents in micronodules were analyzed after picking a lot of micronodules from unit B sediments. REE contents in the collected micronodules are not high compared to those in unit A and B sediments (Fig. 11). Moreover, micronodules have positive value of Ce anomaly while unit B sediments have negative value (Fig. 11). Consequently, enriched REEs in unit B with strong negative Ce anomaly are not considered to be related with the abundant micronodules in unit B. Meanwhile, smectite aggregates abundant in unit B are also not the probable component for the enrichment of REEs in unit B because REE contents in smectite aggregates are very low compared to those in unit B sediments (Fig. 11).

REE contents in smectite are similar to those in unit B (Fig. 11). If unit B sediments are composed mostly of smectite, the smectite would be an important contributor for the enrichment of REEs in unit B. However, unfortunately, we can not do a quantitative analysis of smectite contents in sediments. Although smectite in fine sediments (<2 μm) are the dominant clay minerals in unit B (Fig. 8), it does not mean that the bulk sediments in unit B are mostly composed of smectite.

A lot of white (or water-white) particles are identified to be Ca-P particles (apatite) based on the results of EDS analysis (Fig. 7; welton, 1984; Hein et al., 1979). These particles are fish bones or fish remains (Hein et al., 1979). They make up a major part of the coarse fraction (>25 μm) which can be observed under microscope. REE contents in these particles are more than ten times higher than those in unit A sediments (Fig. 11). Fish remains can be considered to be a probable contributor for the enrichments of REEs in unit B sediments. Meanwhile, Toyoda et al. (1990) reported that a large negative Ce anomaly and enriched REEs in Pacific pelagic sediments are closely related with the abundant fish bone debrises which are composed of biogenic calcium phosphate with abundant REEs and strong negative Ce anomaly.

Low sedimentation rate and high biological activity in the Central equatorial Pacific result in a high contents of fish bone debrises in sediments, which cause a large negative Ce anomaly (Toyoda, 1990). Biological productivity in the central equatorial Pacific was reported to be high during the latest Miocene to the early Pliocene (Leinen and Stakes, 1979). Enriched REEs just below the color boundary, which is the hiatus between the late Miocene to the Pliocene, are considered to be the result of increased input of fish bone debrises produced abundantly during the formation of the hiatus.

V. Summary and Conclusion

Enhanced bottom currents during the late Miocene to the Pliocene, which produced the hiatus of the color boundary between unit A and B, are closely related with the glaciation of Antarctica. The glaciation could result in a steep temperature gradient on earth surface and intensified flows of north and south equatorial currents as well as equatorial counter current. Hence, productivity in the water column during the late Miocene was probably increased, and a large amounts of fish bones and skeletons enriched in REEs were supplied to the seafloor. Moreover, strong bottom currents during the hiatus period are considered to have promoted the reworking and winnowing action and concentrated the coarse grains at the hiatus layer of the upper part of unit B (Jung et al., 1996).

From the above, it is concluded that the enriched REEs in the upper part of unit B were due to the fish remains abundant just below the color boundary. Abundant supply of the remains were probably due to the great changes in paleoceanography (i.e., paleo-climatology) during the formation of the hiatus.

VI. References

Addy, S.K., 1978. Distribution of Fe, Mn, Cu, Ni and Co in coexisting manganese nodules and micronodules. Mar. Geol. 28:M9-M17.

Elderfield, H., C.J. Hawkesworth, M.J. Greaves, and S.E. Calvert. 1981a. Rare earth element zonation in Pacific ferromanganese nodules. Geochim. Cosmochim. Acta 45:1231-1234.

Elderfield, H., C.J. Hawkesworth, M.J. Greaves, and S.E. Calvert. 1981b. Rare earth element geochemistry of oceanic ferromanganese nodules and associated sediments. Geochim. Cosmochim. Acta 45:513-528.

Elderfield, H. and E.R. Sholkovitz, 1987. Rare earth elements in the pore waters of reducing nearshore sediments. Earth Planet. Sci. Lett. 82:280-288.

Gordon, A.L. and R.D. Gerard, 1970. North Pacific bottom potential temperature. In: Geological investigations of the north Pacific. Geol. Soc. Amer. Mem., 126:23-29.

Halbach, P., G. Friedrich, and U. von Stackelberg, 1988. The manganese nodule belt of the Pacific ocean. Ferdinand Enke Verlag Stuttgart, 254pp.

Hein, J.R., C.R. Ross, E. Alexander, and H.W. Yeh, 1979. Mineralogy and diagenesis of surface sediments from DOMES areas A, B, and C. In: J.L. Bischoff and D.Z. Piper (Editors), Marine geology and oceanography of the Pacific manganese nodule province. Plenum Press, New York, 365-396.

Henderson, P.. 1984. Rare earth element geochemistry. Elsvier, 510pp.

Jeong, K.S., J.K. Kang, and S.K. Chough, 1994. Sedimentary processes and manganese nodule formation in the Korea Deep Ocean Study (KODOS) area, western part of Clarion-Clipperton fracture zones, northeast equatorial Pacific. Mar. Geol. 122:125-150.

Johnson, D.A., 1972. Ocean-floor erosion in the equatorial Pacific. Geol. Soc. Amer. Bull. 83:3121-3144.

Jung, H.S., K.S. Jeong, K.Y. Lee, J.K. Kang, and M.Y. Jung, 1990. Origin of manganese nodules and their distribution in the KODOS-89 area, northeastern equatorial Pacific. J. Oceanol. Soc. Korea, 25:189-204.

Jung, H.S., J.K. Kang, K.S. Jeong, and D.H. Shin, 1991. Geochemical characteristics of light yellow brown surface sediments and dark brown colored subsurface sediments in KODOS-89 area, western part of Clarion-Clipperton fracture zone in north Pacific. J. Oceanol. Soc. Korea, 26:193-203.

Jung, H.S., K.S. Kim, D.H. Shin, and S.B. Chi, 1993. Comparison of two methods in grain-size analysis: SediGraph and MasterSizer. J. Oceanol Soc. Korea, 28:72-78.

Jung, H.S., 1994. Geochemistry of sediments, pore waters, and manganese nodules in KODOS area, western part of Clarion-Clipperton fracture zone in the north Pacific. Ph.D. thesis, Seoul Nat'l Univ..

Jung, H.S., 1994. Geochemistry of sediments, pore waters, and manganese nodules in KODOS area, western part of Clarion-Clipperton fracture zone in the north Pacific. Ph.D. thesis, Seoul Nat'l Univ., 282pp.

Jung, H.S, K. S. Jeong, C. B. Lee, and J. K. Kang, 1996. Geochemical and mineralogical properties in two-colored core sediments from the Korea Deep Ocean Study (KODOS) area,

NE equatorial Pacific. Mar. Geol., (in press).

Kadkho, D., 1985. Late Cenozoic sedimentation and metal deposition in the north Pacific. Geochim. Cosmochim. Acta 49:651-661.

Kitano, Y. and R. Fujiyoshi, 1980. Selective chemical leaching of cadmium, copper, manganese and iron in marine sediments. Geochem. J., 14:113-122.

KORDI, 1991. A study on the strategy for the development of deep seabed mineral resources (cruise report). 1101pp.

Lee, K.Y., J.W. Moon, J.K. Kang, H.S. Jung, and S.B. Chi, 1992. Occurrence and distribution of manganese nodules in KODOS-89 area, northeast Pacific. J. Oceanol. Soc. Korea, 27:210-227.

Leinen, M. and D. Stakes, 1979. Metal accumulation rates in the central equatorial Pacific during Cenozoic time. Geol. Soc. Am. Bull., 90:357-375.

Muller, P.J. and A. Mangini, 1980. Organic carbon decomposition rates in sediments of the Pacific manganese nodule belt dated by Th-230 and Pa-231. Earth Planet. Sci. Lett., 51:94-114.

Munsell, 1988. Soil color chart. McBeth Div., Kolmorgen Corp., Mayland.

Murray, R.W., M.R.B. Brink, H.J. Brumsack, D.C. Gerlach and G.P. Russ III, 1991. Rare earth elements in Japan sea sediments and diagenetic behavior of Ce/Ce*: Results from ODP Leg 127. Geochim. Cosmochim. Acta 55:2453-2466.

Piper, D.Z.. 1974. Rare earth elements in ferromanganese nodules and other marine phases. Geochim. Cosmochim. Acta 38:1007-1022.

Piper, D.Z. and M.E. Williamson, 1977. Composition of Pacific ocean ferromanganese nodules. Mar. Geol., 23:285-303.

Piper, D.Z. and J.R. Blueford, 1982. Distribution, mineralogy, and texture of manganese nodules and their relation to sedimentation at DOMES site A in the equatorial north Pacific. Deep-Sea Res., 29:927-952.

Piper, D.Z., P.D. Rude, and S. Monteith, 1987. The chemistry and mineralogy of haloed burrows in pelagic sediment at DOMES site A: The equatorial north Pacific. Mar. Geol., 74:41-55.

Skornyakova, N.S. and I.O. Murdmaa, 1992. Local variations in distribution and composition of ferromanganese nodules in the Clarion-Clipperton nodule province. Mar. Geol., 103:381-405.

Toyoda, K., Y. Nakamura, and A. Masuda. 1990. Rare earth elements of Pacific pelagic sediments. Geochim. Cosmochim Acta 54:1093-1103.

Savin, S.M., R.G. Douglas, and F.G. Stehli, 1975. Tertiary marine paleotemperatures. Geol. Soc. Am. Bull. 86:1499-1510.

van Andel, T.J., G.R. Heath, and T.C. Moore,Jr., 1975. Cenozoic history and paleoceanography of the central equatorial Pacific ocean. Geol. Soc. Am. Mem., 143:1-134.

von Stackelberg, U., 1982. Influence of Hiatuses and volcanic ash rains on the origin of manganese nodules of the equatorial north Pacific (Valdivia cruises VA-13/2 and VA-18). Mar. Mining, 3:297-314.

Welton, J.E., 1984. SEM petrology atlas. AAPG, 237pp.

Table 1 Summary of station numbers and the depth of color boundary in box core sediments from KODOS-92 sites. Unit of C.B. depth is is "cm", and "-" means that unit A occurs only in the core sediments without the color boundary.

Station No.	1	5	14	23	27	29	34	36	37	38
Depth of C.B.	-	-	30	-	-	-	25	18	25	-

. C.B. : color boundary

Table 2 Summary of sediment characteristics in unit A and B sediments from KODOS-90 site

Sediment characteristics	***unit A***	***unit B***
Sediment color	brown ~ pale brown	dark brown
Age	Quaternary	Tertiary
Preservation state of siliceous fossils	fairly well preserved	severely corroded
Contents of micronodules, smectite aggregates	rare	abundant
Occurrence of fish remains (spicules, spines, and fish bone debrises	rare	abundant
Contents of metals (Mn, Cu, Ni, REEs)	low	high

Table 3 Contents of REEs in box core sediments from KODOS-90 sites. All units of depth and REEs contents are "cm" and "ppm", respectively.

St.1

Depth	La	Ce	Pr	Sm	Eu	Gd	Dy	Ho	Er	Tm	Yb	Lu
0	31	60	11 9	11 8	3 3	12 8	12.3	2 5	6 8	0 92	6 1	0.89
1	31	56	11.1	11 9	3 3	13 1	11.1	2 3	6.1	0.84	5.4	0.80
2	26	54	10.1	10.8	2.8	11.4	9.8	2 0	5.4	0.72	4.6	0.67
3	24	50	9.1	10 3	2.8	10 9	10.2	2.1	5.6	0.81	5 2	0.75
4	19	40	6 9	7 2	2 4	9 0	8.0	1.7	4 6	0 63	4.2	0.60
6	15	39	7 1	8.4	2.4	9 7	8.9	1.8	4.9	0.70	4 6	0.64
8	19	46	7.7	8 8	2 4	9 9	9 3	1 9	5.3	0 76	5.0	0.73
10	12	28	4 8	5.5	1 6	6 3	6 1	1 3	3.5	0.52	3 3	0 49
13	12	30	5 0	5.3	1 6	6.1	6 2	1 3	3.6	0.51	3.4	0.50
16	15	36	6 3	7.3	2 0	8 1	8.0	1 7	4.7	0.66	4.4	0.63
20	17	42	7 8	8 7	2 5	9 9	9 2	1.9	5 4	0.74	4 8	0 72
25	19	45	8 1	9 5	2 7	10 7	10 2	2.0	5 6	0.81	5.3	0 78
30	23	51	9.5	10 7	2.9	11.7	10 3	2 1	5 9	0.82	5 3	0 78
35	12	30	5.1	6.4	1.9	7.2	7.3	1.6	4.4	0.62	4.2	0.63
40	11	29	4.8	5.6	1.7	6.6	6 6	1 3	3 9	0.56	3 7	0 55
50	13	32	5 7	6.5	1 9	7.8	7 4	1 5	4 3	0 61	4.0	0.58

St.5

Depth	La	Ce	Pr	Sm	Eu	Gd	Dy	Ho	Er	Tm	Yb	Lu
0	17	41	7.1	7 6	2.1	8.5	8.6	1 8	5.1	0.73	4.9	0.73
1	12	30	4 8	5 3	1 5	6 0	6 0	1 2	3 5	0 49	3 3	0 48
2	16	37	6 1	6 4	1.8	7 2	7.3	1 5	4 3	0.61	4.1	0.60
3	12	30	5 0	5 2	1.5	6.1	6.6	1.4	4 0	0.58	3 9	0.58
4	14	34	5 5	5.9	1.8	6 9	7.1	1 5	4 2	0.60	4.1	0.59
6	13	34	5.3	5 9	1 7	6.6	6.8	1.4	4.0	0.56	3.8	0.56
8	15	35	5 4	5 3	1.5	5 9	6 1	1.3	3.6	0.51	3.5	0.51
10	14	35	5.2	5.2	1.6	6 0	6.0	1 3	3.5	0.50	3.4	0 49
13	15	37	5.6	6 0	1.7	6.5	6.5	1 3	3.7	0.51	3.4	0.50
16	14	31	5 2	5 4	1.5	6.0	6 0	1.2	3 4	0.49	3 3	0.47
20	18	41	7.7	8.6	2 4	9 2	9.2	1.9	5.3	0.75	5.2	0.74
25	12	32	4.9	5.4	1.6	6.0	6.3	1.3	3.6	0.53	3.5	0.51
30	19	46	8 2	9.1	2.8	10 1	9.9	2 0	5.7	0.82	5 5	0.80
35	17	40	7 4	8.3	2 5	9.1	9.0	1.9	5.3	0.75	5.1	0.75
40	17	42	7.4	8 1	2 5	8.9	8 6	1 8	4.9	0 68	4.6	0.69
50	17	44	7 2	7 9	2.3	8 5	8 4	1 7	4 8	0 66	4 5	0 65

St.14

Depth	La	Ce	Pr	Sm	Eu	Gd	Dy	Ho	Er	Tm	Yb	Lu
0	40	59	16	18	5.1	21	20	4 1	11.3	1.6	10.5	1 5
1	36	52	15	17	4.9	20	19	3 8	10.5	1.5	9 6	1.4
2	28	48	12	14	4.6	18	16	3.4	9.3	1.3	8.5	1.3
3	24	40	10	12	3 7	15	14	3 0	8 1	1.2	7 5	1.1
4	52	70	20	21	6 1	24	21	4 3	11.8	1.7	10.5	1 6
6	33	54	14	16	4 7	19	18	3 7	10 2	1 5	9 4	1.4
8	21	36	9	12	3 8	15	15	3.1	8.6	1.3	8.2	1.2
10	43	64	17	19	6.0	22	20	4 2	11 3	1.6	10 2	1.6
13	44	65	17	18	5.7	22	19	3 9	10 3	1.5	9.3	1.4
20	32	48	14	17	5 3	21	20	4.3	11 6	1.7	10 7	1.6
25	39	56	16	18	5 9	22	21	4.4	11 9	1 7	10 9	1 7
30	82	73	31	32	9 3	37	33	7 0	18.3	2 6	16.1	2 5
35	154	80	49	47	12 4	53	50	10 8	29 1	4.0	26.0	4.0
40	163	80	50	46	11 9	51	48	10.4	28 6	4.1	26 2	4.0
50	142	73	46	44	11 6	49	46	9 8	26 8	3 8	24.3	3 8

Table 3 (continued)

St.23

Depth	La	Ce	Pr	Sm	Eu	Gd	Dy	Ho	Er	Tm	Yb	Lu
0	40	56	12 5	13 1	3.6	15 1	14.3	2.8	8 2	1.12	7.6	1.06
1	35	51	12.1	13 5	3 5	15 4	14.2	2.9	8 4	1.18	7 9	1.18
2	30	48	10 5	10 7	3 1	11.8	10.8	2 4	6.6	0.91	5.9	0 89
3	23	42	9 4	10 7	3 0	12.3	12.0	2 5	7 0	0.96	6.6	0.96
4	27	45	10 3	10 9	3 0	13 1	12.4	2.7	7 4	0.99	7.1	1 03
6	36	56	12.1	12.8	3 5	13.3	13.7	2.9	7.8	1.14	6 9	1.09
8	19	35	6 8	6 9	2 0	8 4	8.8	1 9	5.0	0.66	4 6	0 68
10	27	44	9 4	9 2	2 7	10 8	10.9	2 4	6 1	0 90	5 8	0 91
13	19	36	6 9	7 5	2 2	7 8	8 2	1 8	4.8	0 71	4.3	0.66
16	17	31	6 3	7 3	2.1	8 5	9 1	1 9	5 2	0 75	5 1	0.78
20	19	33	7 0	8 4	2.3	10.0	10.2	2.1	5 8	0 80	5.4	0.80
25	20	37	7 3	8 3	2.4	9.0	9 2	2.0	5 2	0.78	4.7	0.73
30	27	42	10 9	12 1	3 3	13 5	12 7	2.8	7 6	1.04	7 0	1.06
35	18	34	7 0	7.5	2 1	8 6	8.2	1.8	4 7	0.64	4 1	0.63
40	24	40	9 2	9 7	2.9	11 7	11.4	2 4	6.6	0.95	6 2	0.93

St.27

Depth	La	Ce	Pr	Sm	Eu	Gd	Dy	Ho	Er	Tm	Yb	Lu
0	15	34	6.4	7.4	2.2	8.7	8 6	1 8	5 1	0.71	4 7	0.70
1	18	40	7.9	9 1	2 6	10 5	9.7	2.1	5.7	0.79	5.2	0.77
2	24	46	9.1	9 0	2.6	10.3	9.9	2.1	5.9	0.79	5.4	0.79
3	26	52	10 9	11 6	3 3	12.8	11 8	2.5	6 8	0 94	6 1	0.89
4	14	33	6 0	6.7	1 9	7.7	7 8	1.7	4.7	0.66	4 4	0.64
6	19	45	8.4	9 2	2.9	10.9	9.9	2.1	5.8	0.79	5 2	0.77
8	24	49	10.2	10.9	3.2	12 2	10.8	2.3	6 2	0.86	5 6	0.83
10	17	37	7 2	7.9	2.4	9.4	8.9	1.8	4.9	0 69	4 6	0.69
13	18	39	7.3	7 8	2 4	8 7	8.0	1.7	4 4	0 62	4 1	0 59
16	20	42	8.4	9 2	2.7	10 2	9 6	2.0	5.5	0 76	5.2	0.76
20	23	46	9 1	9 4	2 8	10.7	10.0	2 1	5 6	0.79	5 2	0 78
25	25	53	10 6	10 9	3.5	13.1	10 9	2 3	6.0	0.83	5.4	0.80
30	26	50	10.6	10 9	3 2	12.5	11.1	2 3	6.1	0.86	5 8	0.85
35	31	56	12 5	13 1	4 0	14 5	12.7	2.6	6.9	0.95	6.4	0 92
40	20	38	7.8	8.0	2.6	9.5	8.4	1.8	4.7	0.67	4.4	0.65
50	15	32	5 9	6 2	2.0	7.2	6.8	1.4	3 8	0 55	3 6	0.53

St.29

Depth	La	Ce	Pr	Sm	Eu	Gd	Dy	Ho	Er	Tm	Yb	Lu
0	20	38	8.3	9.6	2.9	11.1	10.4	2.2	6.0	0.82	5.6	0.82
1	20	35	7 3	8 1	2 4	9.2	9 1	2 0	5 4	0.76	4.9	0.75
2	19	35	7 7	8 5	2.5	10.1	10 2	2.1	5 8	0 83	5.6	0.81
3	31	51	10 9	11 2	3 2	12.7	12.2	2 5	6 9	0 95	6.5	0.97
4	21	40	8.8	9 9	2 9	11 6	11 4	2 4	6 5	0.87	5.8	0.87
6	12	27	5 5	7.0	2.3	8 6	9.3	2 0	5 7	0.83	5.7	0.86
8	6	16	2.8	3 9	1.5	5.1	5 9	1 3	3.7	0.55	3.7	0.57
10	20	36	7 4	8 3	2 6	9.6	9.8	2 1	5.8	0.82	5 6	0.82
13	13	27	6 0	7.4	2.4	8 8	9 5	2 0	5.9	0.84	5.7	0.85
16	16	30	6.2	7.3	2.5	8 6	8 6	1.8	4.9	0.67	4.5	0.66
20	14	27	5.4	6 3	2 2	7 9	8.0	1.7	4 7	0.66	4.5	0 66
25	20	37	8 4	9 7	3.1	11.1	10.9	2.3	6.4	0.88	5.9	0.87
30	21	42	9 0	10 4	3.5	11 9	11.4	2 4	6 5	0 91	6 0	0 88
35	21	38	8 8	10 0	3.3	11.8	11.5	2.4	6 6	0.92	6.2	0.90
40	18	32	7.2	8 0	2 7	10.0	10.0	2 1	5.9	0.82	5.6	0.81
50	25	39	9 1	9 8	3 1	11 8	11 6	2 4	6 9	0 97	6 5	0 99

Table 3 (continued)

St.34

Depth	La	Ce	Pr	Sm	Eu	Gd	Dy	Ho	Er	Tm	Yb	Lu
0	18	39	7 7	9 3	3.0	10	10	2.2	5.9	0 85	5.5	0.84
1	19	42	7.9	9 2	2 9	10	10	2 0	5.6	0.80	5 2	0.79
2	19	42	8 0	9 4	3 0	11	10	2.1	5 6	0 80	5.1	0.76
3	21	42	8.1	9 3	3.0	10	10	2 1	6.0	0.87	5.6	0.87
4	20	43	8 4	9 6	3.3	11	10	2 2	6 0	0.88	5.6	0.86
6	17	39	7.4	8 9	2.9	10	10	2 1	5 8	0.82	5.4	0.83
8	19	41	7 8	8 6	3 0	10	10	2 0	5.5	0 79	5 2	0 77
10	27	54	10.7	12 2	3 7	13	13	2 6	7 0	0 97	6.3	0.97
13	30	57	12.2	13 8	4.1	15	14	3.0	8.0	1.10	7.3	1.10
16	45	72	18.1	20.0	5 7	21	20	3 9	10 7	1.45	9.5	1.42
20	38	50	16.2	18.9	5 7	22	21	4.5	12.6	1.73	11 4	1.72
25	74	72	26.9	28.5	8.5	32	30	6.4	17.6	2 44	16 0	2.42
30	115	76	35.6	33.5	8 7	38	36	7.7	21.6	2.99	19.2	2.94
35	101	74	32.5	31.0	8 0	34	32	6.8	19.1	2.60	16.8	2 56
40	97	75	30 0	28 2	7.1	31	28	6.1	17.1	2 30	14 8	2.25

St.36

Depth	La	Ce	Pr	Sm	Eu	Gd	Dy	Ho	Er	Tm	Yb	Lu
0	51	59	21	23	6 3	26	24	5 0	14	1.9	13	1.9
1	57	67	23	24	6.8	27	24	5.0	14	1.9	12	1.8
2	58	69	23	25	6.7	27	24	5.0	14	1.9	12	1.8
3	45	58	18	21	5.5	23	21	4 4	12	1 7	11	1.7
4	44	57	18	21	5.5	22	21	4.3	12	1.6	11	1.6
6	49	63	20	22	6.2	24	22	4.5	13	1.8	11	1.7
8	59	70	23	23	6.6	26	24	4 8	13	1.9	12	1.8
10	45	66	19	21	5.9	23	21	4 2	12	1 6	11	1 5
13	84	80	30	29	8 3	32	29	5.8	16	2.2	14	2 0
16	78	76	28	28	7 6	31	28	5.7	16	2.2	14	2.1
20	125	72	41	39	9.7	43	38	8.0	23	3.1	20	2.8
25	122	69	42	40	10 0	44	40	8.5	23	3.2	20	3.0
30	133	77	43	41	10.3	45	41	8.6	24	3.3	21	3.1
35	127	71	41	39	9.9	43	40	8.3	24	3.2	20	3.0
40	126	72	42	39	9.8	43	40	8.4	24	3.2	21	3.0

St.37

Depth	La	Ce	Pr	Sm	Eu	Gd	Dy	Ho	Er	Tm	Yb	Lu
0	39	51	15	16	4.3	17	16	3 3	8.8	1.3	7.9	1 2
1	32	47	13	15	4.2	16	16	3.3	9 0	1.3	8.2	1.2
2	28	43	12	13	3.7	14	14	2.8	7.5	1.1	6.9	1.0
3	42	57	16	17	4.4	18	16	3.5	9.5	1.3	8.2	1.2
4	35	50	14	16	4.5	18	17	3.4	9.4	1.3	8.7	1.3
6	38	53	15	18	5.0	19	18	3.8	10.2	1.4	9.5	1.4
8	35	51	14	16	4 2	17	16	3.5	9 2	1.3	8.5	1.3
10	30	41	11	13	3 6	14	13	2 8	7.7	1.1	6.9	1 0
13	29	39	11	13	3.7	14	14	3.0	8 2	1.1	7.3	1 1
16	29	41	11	14	4.1	15	16	3.3	9.1	1.3	8.3	1.2
20	29	45	12	13	3 9	15	14	3.0	8 0	1.1	7.1	1.0
25	56	55	22	25	6.8	26	25	5.2	14.1	2.0	12.9	1.9
30	105	75	39	38	10.1	40	37	7.8	20 6	2.8	17.7	2 6
35	110	76	38	37	9 6	40	36	7 3	19.5	2.6	17 1	2.5
40	106	74	36	35	8.8	36	33	6 7	18.3	2 5	15 8	2 3

Table 3 (continued)

St.38

Depth	La	Ce	Pr	Sm	Eu	Gd	Dy	Ho	Er	Tm	Yb	Lu
0	22	44	8.7	9.2	2.5	9.7	8.8	1 8	5.0	0.66	4.4	0.62
1	24	50	9 9	10 1	2 7	10.9	10 2	2.0	5.6	0.75	5.0	0.73
2	15	33	6.3	7 1	1.9	7.5	7.2	1.5	4.3	0.56	3.8	0.54
3	27	53	10 6	11.0	2.9	11.6	10.6	2.0	5.8	0 76	5.1	0.74
4	17	40	6.9	7.6	2.0	8.1	8.0	1.6	4.5	0.62	4 0	0.57
6	25	51	10 0	10 1	2 8	10 8	9 8	2.0	5.5	0.74	4.9	0.70
8	20	42	7.4	7 4	2 1	8 0	7.5	1.5	4.4	0.58	3.8	0.55
10	17	38	6 8	7 1	2.0	7.6	7.1	1.5	4.1	0.54	3.6	0.50
13	17	36	6.8	7.3	2 0	7.6	7 3	1 5	4.2	0.57	3.7	0.53
16	21	44	7 8	7.9	2.3	8.9	8 4	1 7	4 9	0 67	4.4	0.62
20	24	48	9 8	10 6	2 8	11 2	10 1	2.0	5.6	0.74	4.9	0.70
25	33	61	12 3	12.5	3.3	12.8	11.7	2.4	6.7	0.89	5 8	0.83
30	34	61	13.7	14 3	3.8	15 0	13 5	2 7	7.3	0.97	6.4	0.92
35	17	35	6 8	7.7	2.3	8.9	8.7	1.7	5.1	0.67	4.5	0.66
40	30	57	12.6	13 8	3 6	14.1	12.9	2.6	7.3	0.93	6.1	0.84
50	31	52	11.1	10.9	2.9	11 6	10.9	2.1	6.2	0 8	5.4	0.78
60	22	41	8.3	8 9	2 4	9.4	8 8	1 7	5.0	0 66	4.4	0.63

Table 4 Statistical (maximum, minimum, average) and normalized values of REE contents in box core sediments from KODOS-91 sites.

	La	Ce	Pr	Sm	Eu	Gd	Dy	Ho	Er	Tm	Yb	Lu
Maximum	163	80	50	47	12	53	50	11	29	4	26	4
Minimum	6.2	16.4	2.8	3.9	1.5	5.1	5.9	1.2	3.4	0.5	3.3	0.5
Max./Min.	26	5	18	12	9	10	8	9	8	8	8	8
Average	35.2	47.8	13.2	13.9	3.9	15.5	14.7	3.0	8.4	1.2	7.6	1.1
NASC	32	73	7.9	5.7	1.24	5.2	5.54	1.04	3.4	0.5	3.1	0.48
Aver./NASC	1.1	0.7	1.7	2.4	3.2	3.0	2.6	2.9	2.5	2.3	2.5	2.4

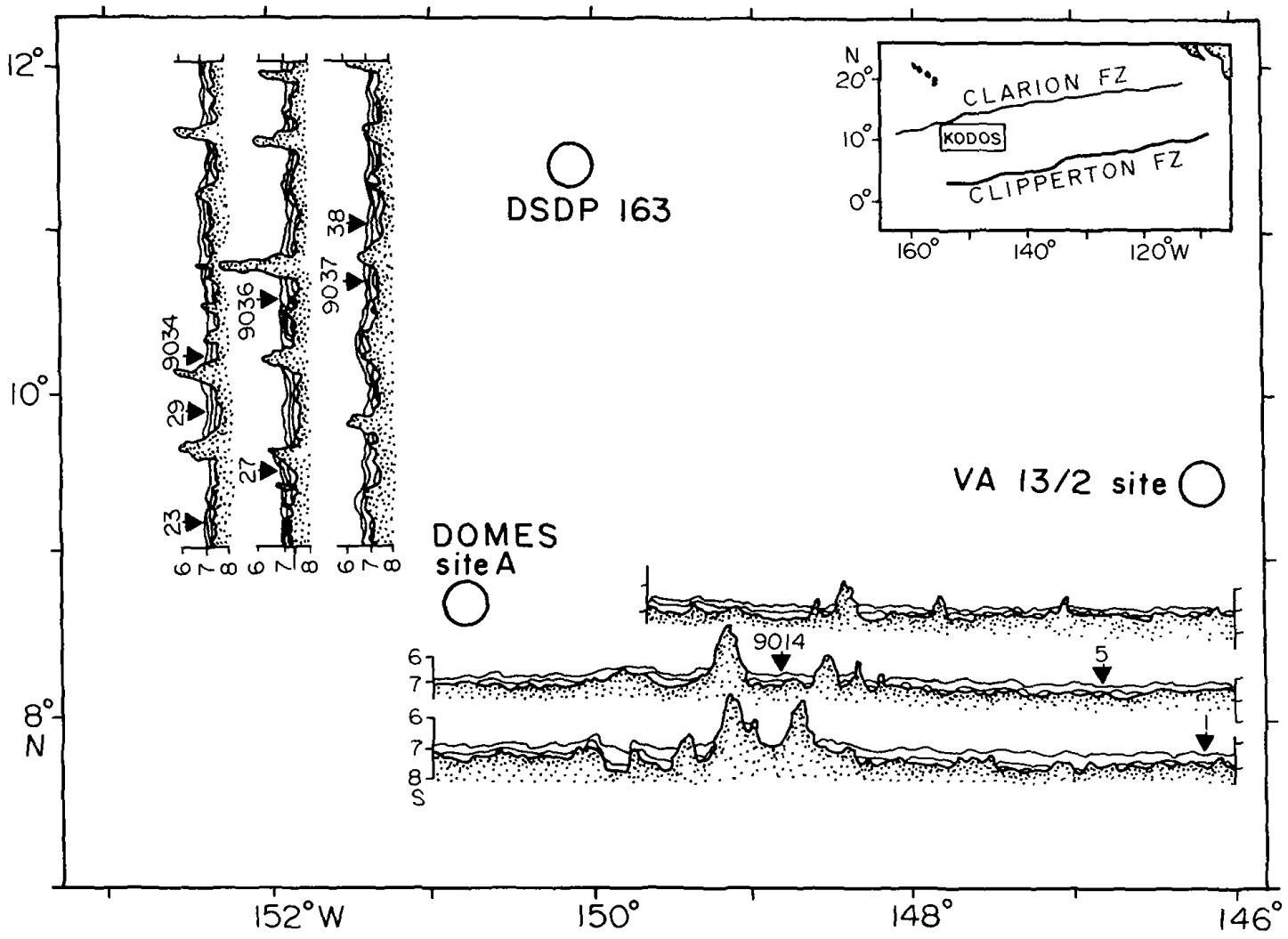

Fig. 1 Sampling stations, seafloor morphology, and sedimentary sequence above acoustic (air-gun) basement in KODOS-90 site

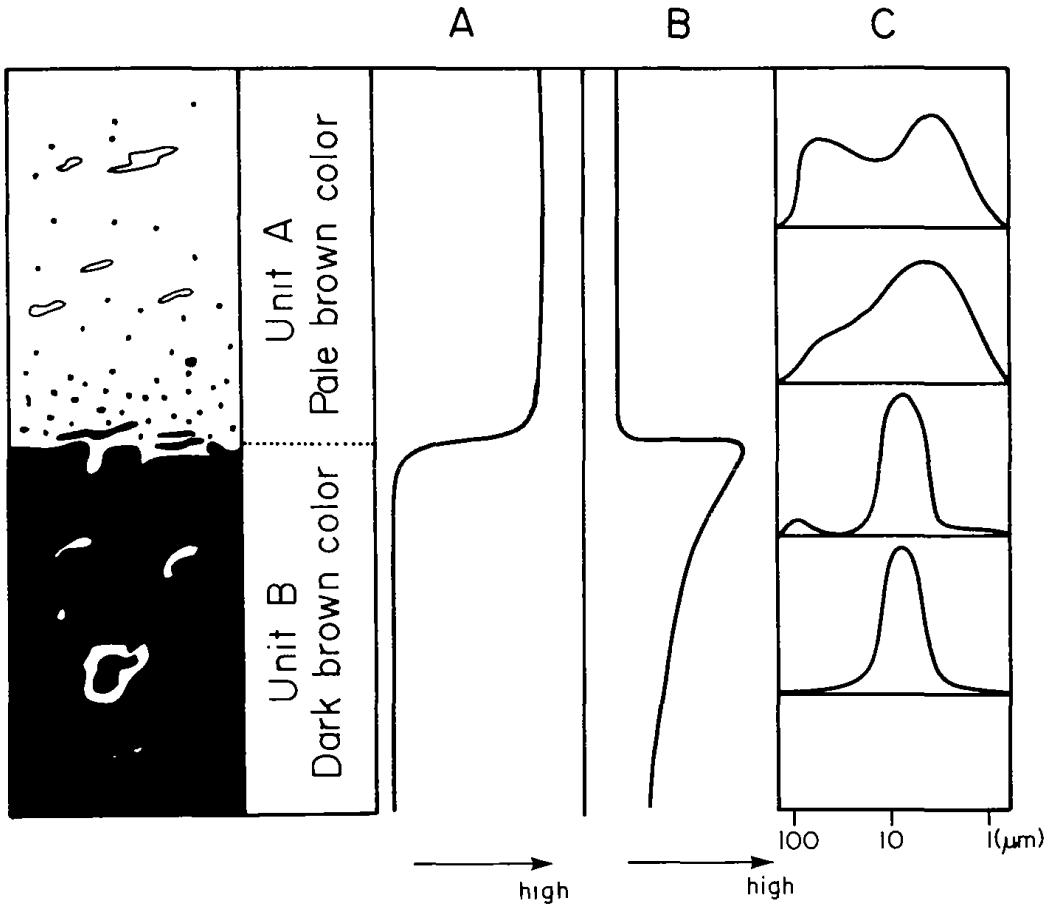

Fig. 2 Schematic diagram showing the vertical variation of sediment characteristics across the color boundary (A: ratio of Quaternary/Tertiary radiolaria, ^{230}Th activity, content of illite, B: contents of smectite, heavy metals (Mn, Cu, Ni), smectite aggregates, micronodules, and fish remains, C: grain size distribution)

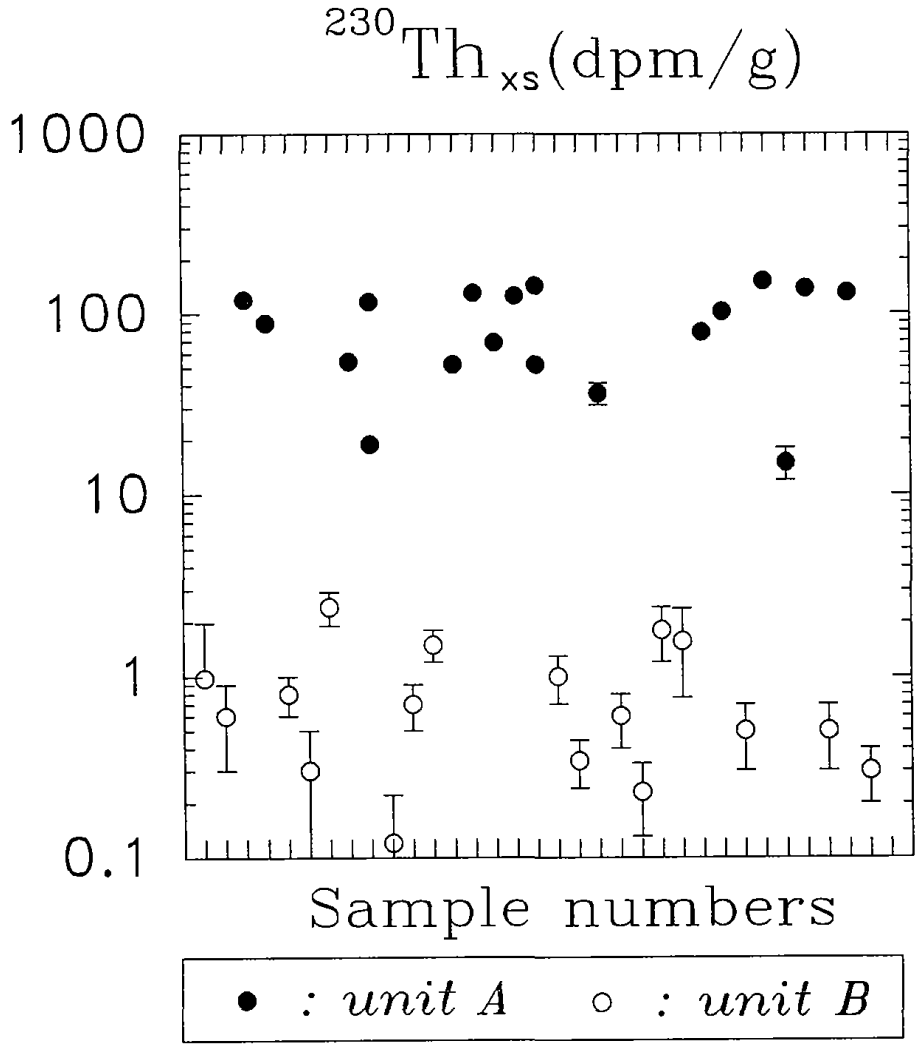

Fig. 3 Excess activities of ^{230}Th in unit A and B sediments from KODOS-90 site

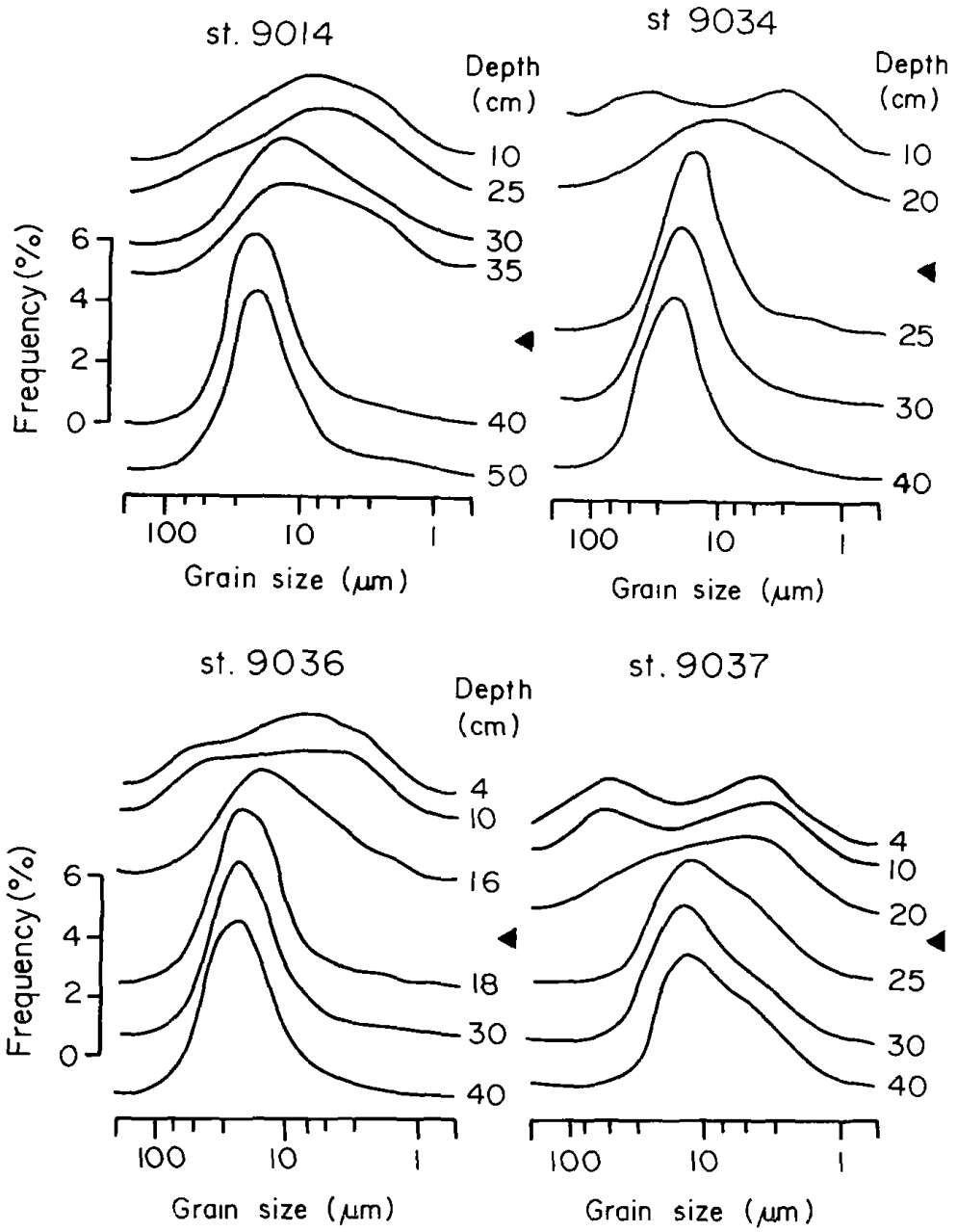

Fig. 4 Grain size distribution of box core sediments from KODOS-90 site. Filled triangle represents the color boundary

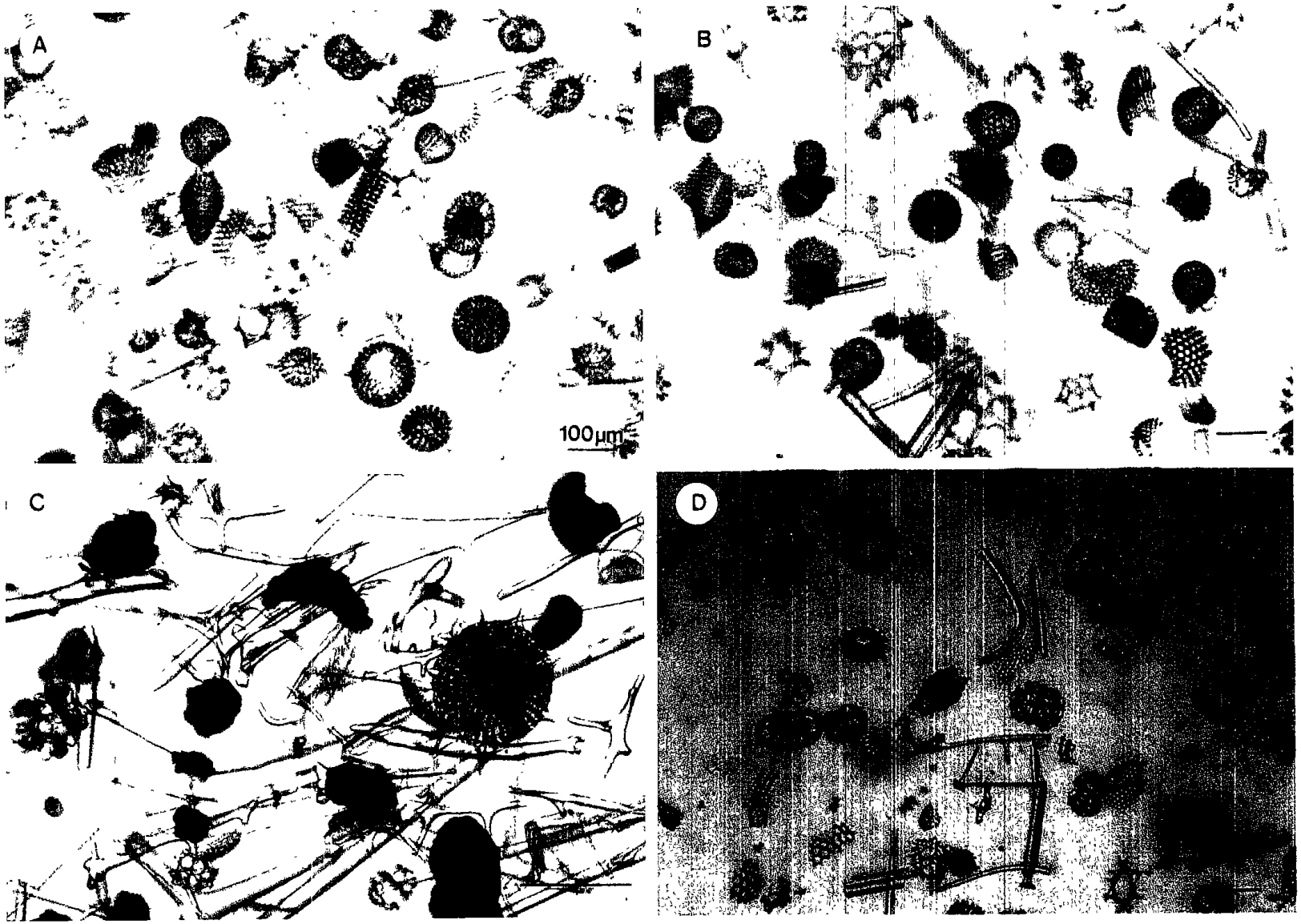

Fig. 5 Photographs showing the features of coarse grains in box core sediments from KODOS-90 site; a) upper part of unit A, b) lower part of unit A, c) upper part of unit B (just below the color boundary), d) lower part of unit B

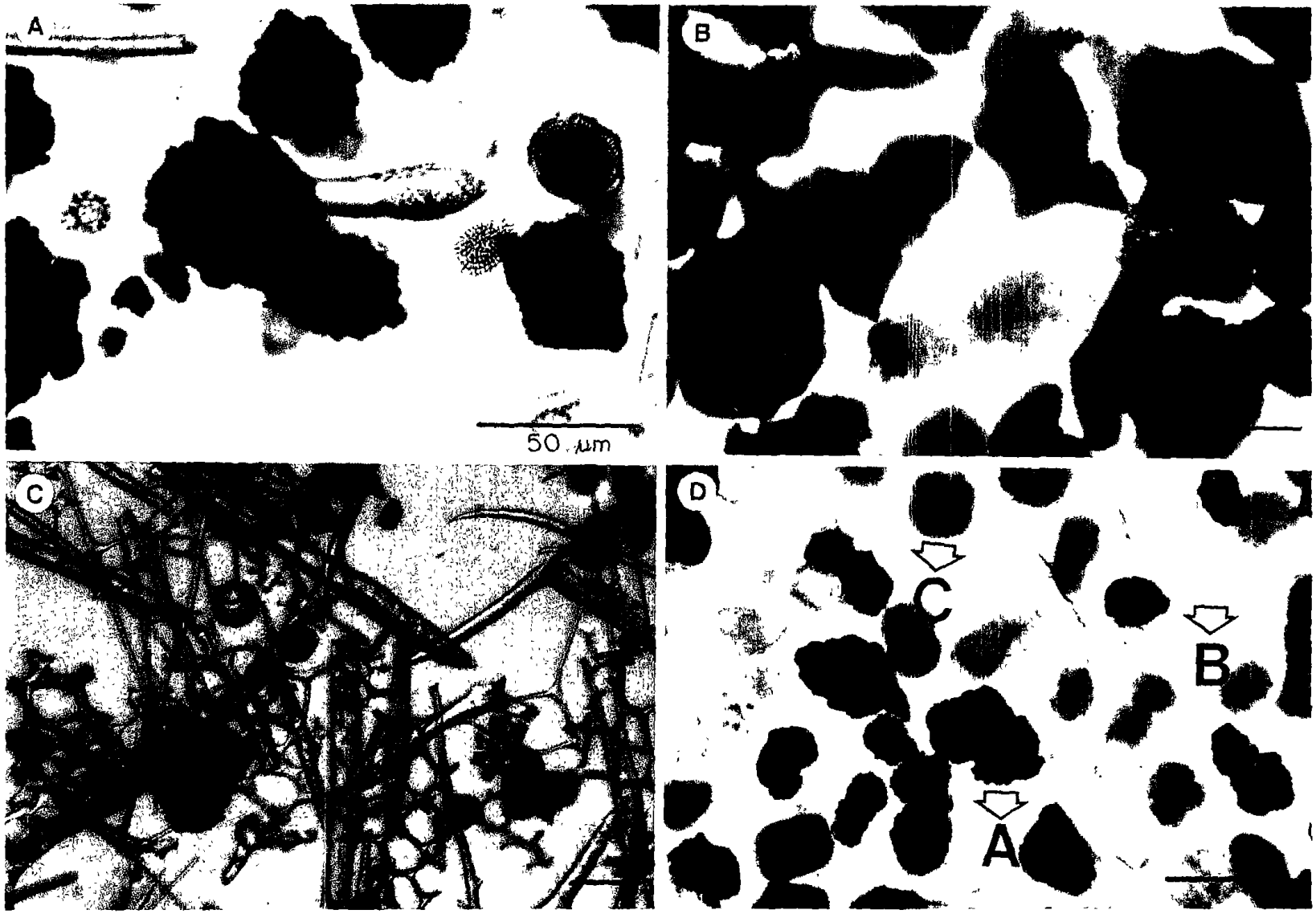

Fig. 6 Coarse grains typically observed in the upper part of unit B sediments. Black (A), brown (B), and white (C) grains represents micronodules, smectite aggregates, and fish remains, respectively.

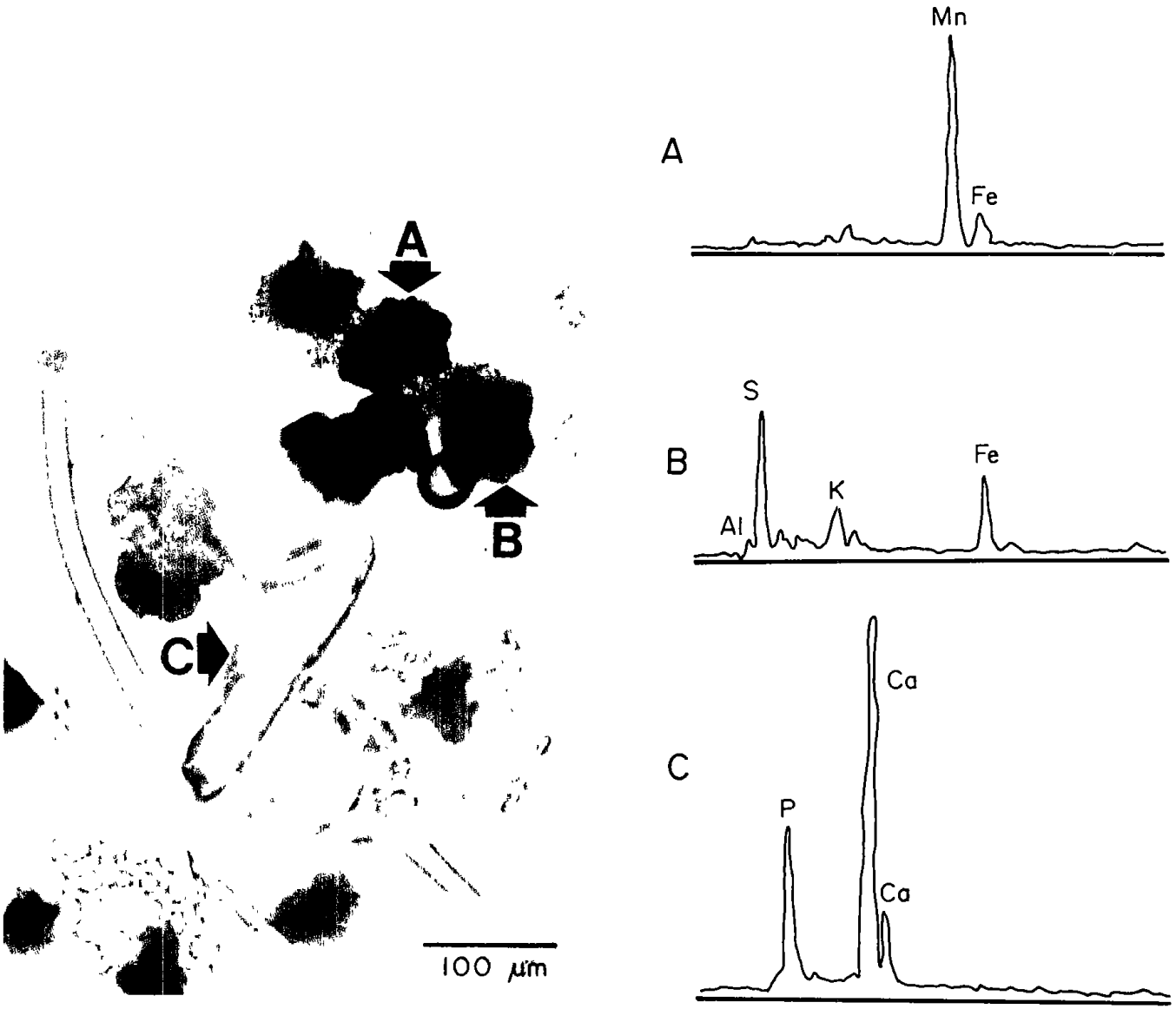

Fig. 7 EDS spectrum for the micronodule (A), smectite aggregate (B), and fish remain (C)

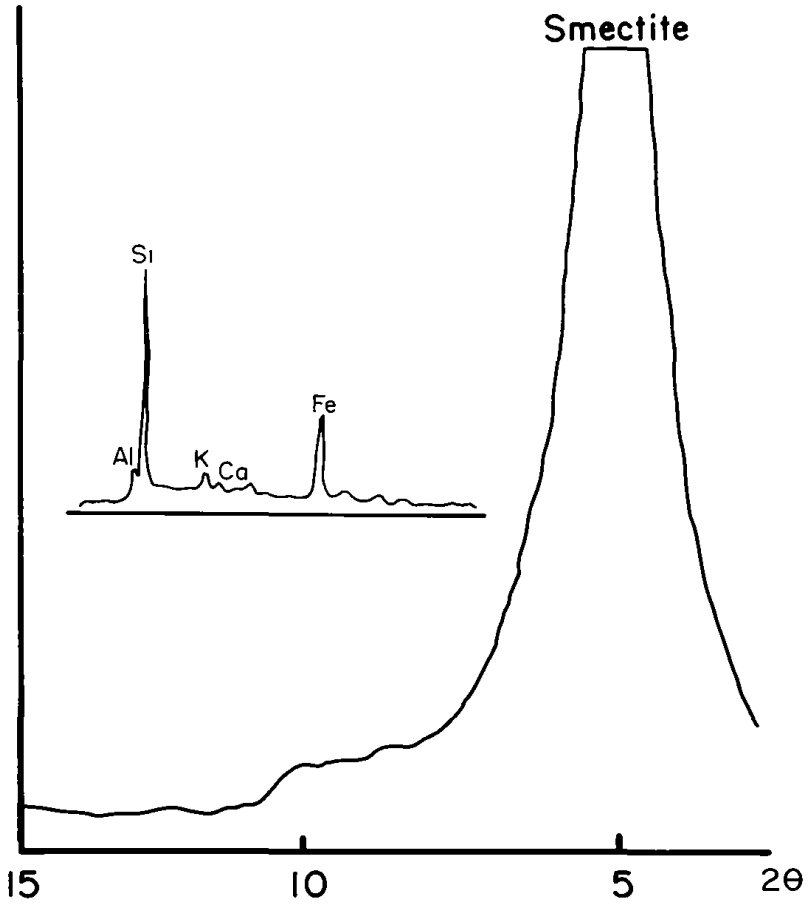

Fig. 8 X-ray diffractogram with a large smectite peak, and EDS spectrum with high Si and Fe peaks in fine sediments (<1 μm) at St.37

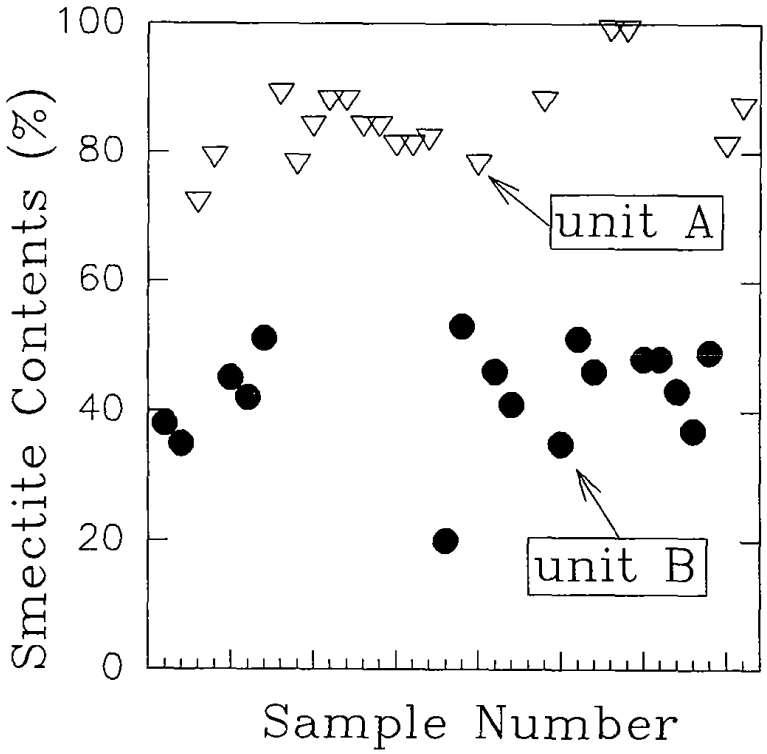

Fig. 9 Contents of smectite in fine fraction (>2 μm) of unit A (filled circle) and unit B (open triangle) sediments in KODOS- 90 site

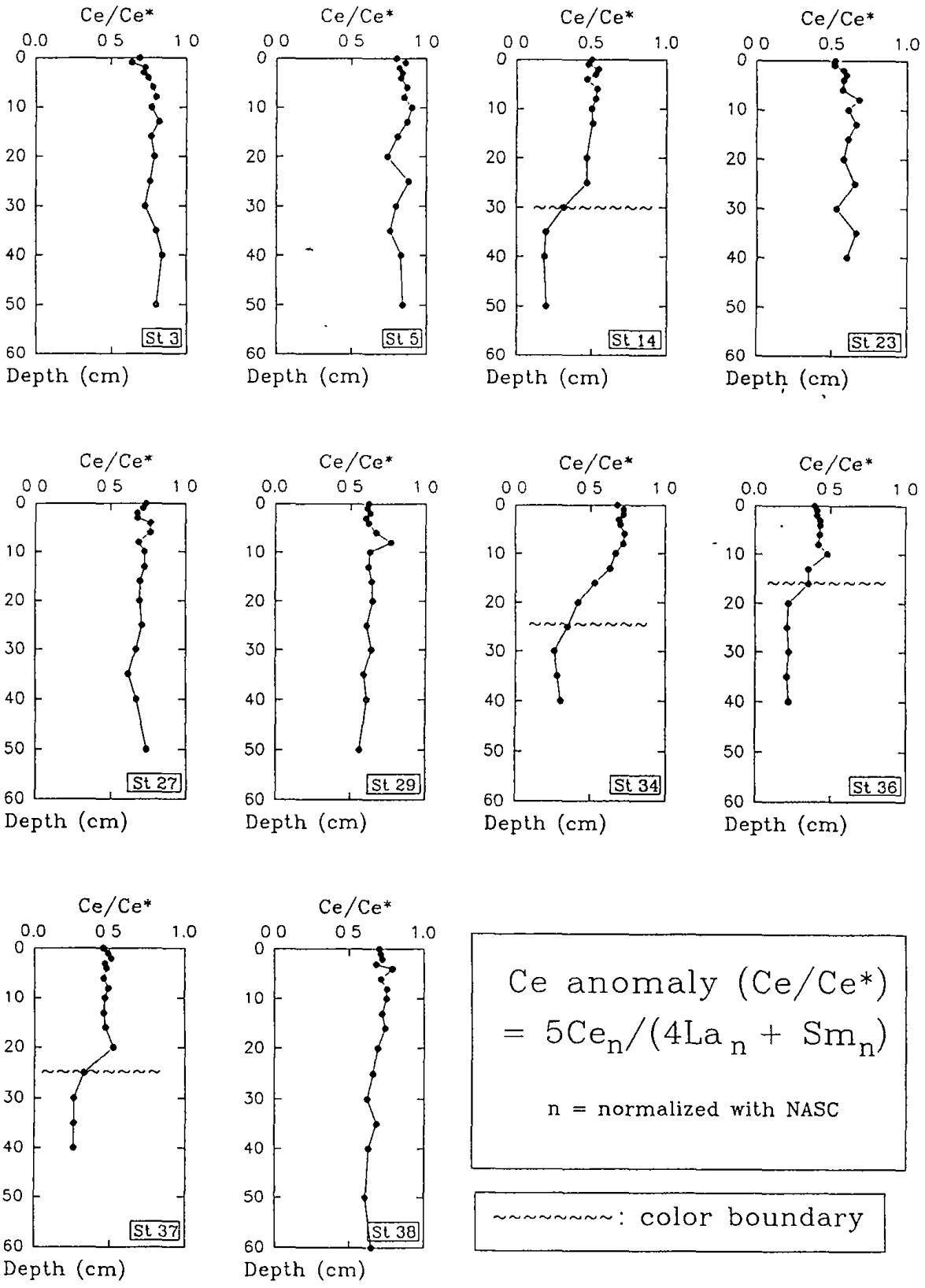

Fig. 10 Depth profiles of Ce anomalies (Ce/Ce*) in box core sediments from KODOS-90 site. Ce/Ce* values decrease abruptly across the color boundary in st.14, st.34, st.36, and st.37

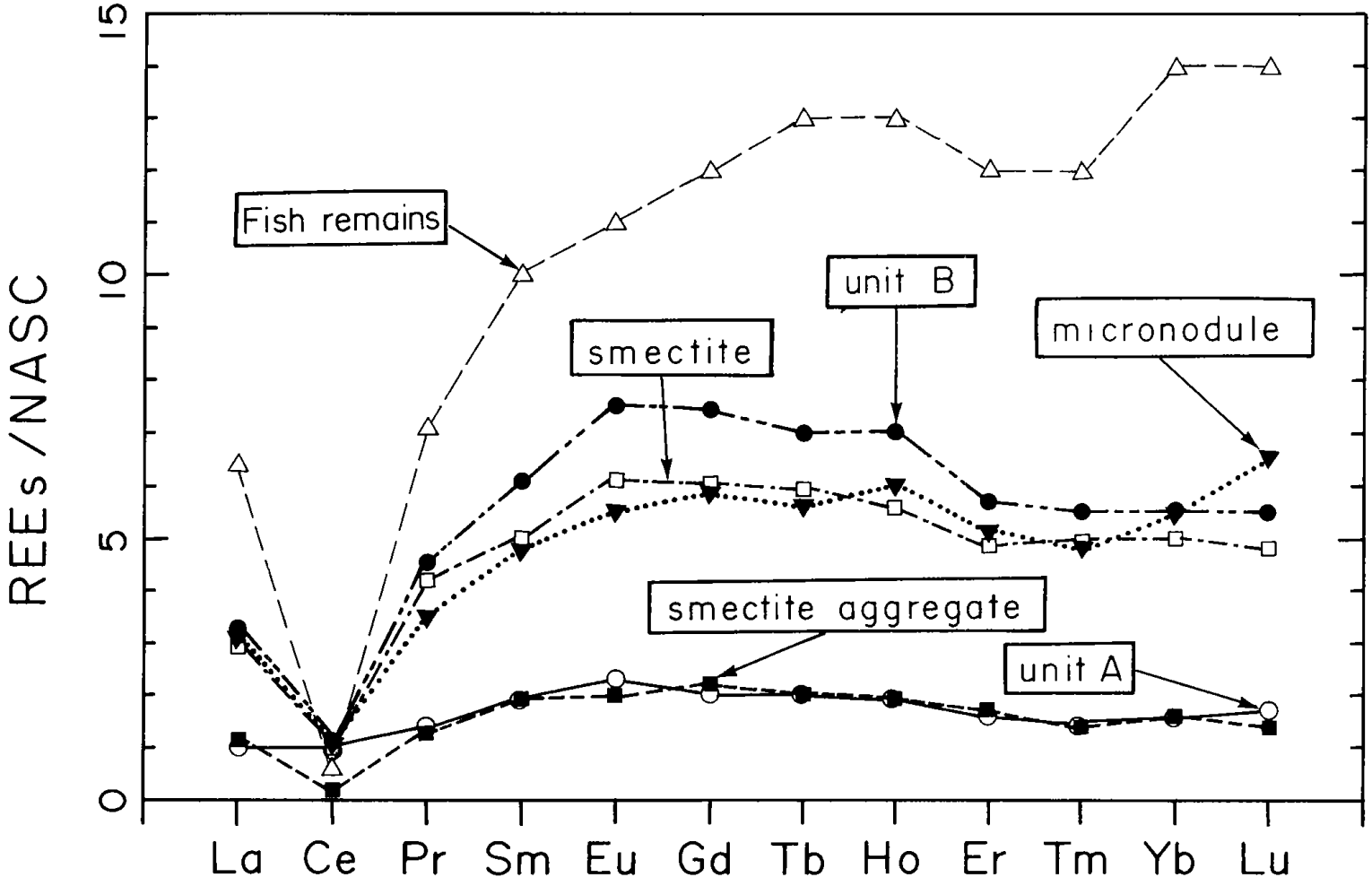

Fig. 11 REE contents in unit A, unit B, smectite, micronodules, smectite aggregates, and fish remains in box core sediments from KODOS-90 site. Note the enriched REEs in fish remains.